PUBLICATIONS OF THE ASTRONOMICAL SOCIETY OF THE PACIFIC
98:1325-1328, December 1986

PHOTOMETRIC OBSERVATION AND ANALYSIS OF THE CLOSE BINARY SYSTEM BO PEGASI

ATSUMA YAMASAKI*†

Department of Earth Science and Astronomy, University of Tokyo, Meguro-ku, Tokyo 153, Japan

AND

AKIRA OKAZAKI*†

Department of Mathematics, Tsuda College, Kodaira, Tokyo 187, Japan

Received 1986 July 24, revised 1986 September 11

ABSTRACT

Photoelectric *BV* light curves of the close binary system BO Peg ($P = 0^{d}.580$) are obtained and analyzed with a synthesis method to determine the photometric elements. It is found that the components of BO Peg are not in contact with each other but almost fill their respective Roche lobes. Two spectrograms of the system (A7 IV–V) have also been obtained, and a brief discussion on physical quantities of the components is made.

Key words: close binary–photometry–light-curve analysis

I. Introduction

The eclipsing binary BO Pegasi was first discovered by Hoffmeister (1935). Jensch (1935) presented the photographic light curve and determined the orbital period to be $0^{d}.58044$. The spectral type was given as A4 in the *General Catalogue of Variable Stars* (Kukarkin *et al.* 1971). No photoelectric light curves have been published so far.

In this study, we present photoelectric *BV* light curves, analyze the light curves, determine a new spectral type from our spectrograms, and discuss briefly the physical properties of BO Peg.

II. Photoelectric Observations

We made photoelectric observations of BO Peg with the 0.6-m reflector of the University of Hawaii at Mauna Kea Observatory on six nights in September 1984. We employed the Tinsley-Goguen photometer with a refrigerated photomultiplier RCA C 31034A(GaAs) and Apple Data System (Goguen 1984). Most of the observations were carried out in *B* and *V*, and a few observations in *U* were also made. The filters used are very similar to those of Johnson's *UBV* standard system.

Two nearby field stars were respectively chosen as the comparison star and the check star. The observations showed no appreciable variations in differential magnitudes between the comparison star and the check star. Table I gives the positions, magnitudes, and color indices of the comparison star and the check star as well as BO Peg at maximum.

We secured the time of the primary minimum, HJD2445969.8604 with $(O-C) = -0^{d}.0399$ from the ephemeris Min. I = HJD2427655.460 + 0.5804342 E (Whitney 1957). Table II lists available observed times of minima of BO Peg, including the present one. From these 28 minima, we derived the ephemeris Min. I = HJD2445969.8709 + 0.58043326 E, by using the least-squares method with weights 1, 3, and 10 for visual, photographic, and photoelectric observations, respectively. The $(O–C)$ values calculated from the latter ephemeris are given in the third column of Table II and are plotted in Figure 1. It is found that neither the ephemeris of Whitney (1957) nor the revised one satisfies the present light variations of BO Peg: the two opposite trends in the $(O–C)$ diagram around $E = -20{,}000$ and 0 suggest that period changes may have occurred. We need more photoelectric observations.

Differential magnitudes ΔV, ΔB, and ΔU, in the sense

TABLE I

Positions, Magnitudes, and Color Indices of BO Peg, Comparison Star, and Check Star

Star	RA(1950)	Dec(1950)	V	B - V	U - B
BO Peg	$21^{h}28^{m}54^{s}$	$+11^{\circ}43'.6$	11.90*	+0.36*	+0.10*
Comparison	21 29 26	+11 41.9	9.73	+0.51	+0.07
Check	21 29 36	+11 39.9	9.87	+0.50	+0.02

* At maximum light.

*Guest Observer, Mauna Kea Observatory, Institute for Astronomy, University of Hawaii.

†Observations were partially made at Okayama Astrophysical Observatory.

TABLE II

Observed Times of Primary Minima and Their (O-C) Values

HJD2400000+	E	O-C*	Method	Source**
26223.531	-34020	0d000	pg	1
26244.392	-33984	-0.035	pg	1
26333.238	-33831	+0.005	pg	1
27655.450	-31553	-0.010	vis	1
27658.362	-31548	0.000	vis	1
27666.500	-31534	+0.012	vis	1
27684.490	-31503	+0.008	vis	1
27685.630	-31501	-0.013	vis	1
27688.547	-31496	+0.002	vis	1
27691.450	-31491	+0.003	vis	1
27699.580	-31477	+0.007	vis	1
27745.426	-31398	-0.001	vis	1
32005.793	-24058	-0.015	pg	2
32799.842	-22690	+0.002	pg	2
33584.599	-21338	+0.013	pg	2
33981.612	-20654	+0.010	pg	2
34245.705	-20199	+0.006	pg	2
34627.642	-19541	+0.017	pg	2
35002.600	-18895	+0.016	pg	2
44194.337	-3059	+0.011	vis	3
44201.296	-3047	+0.005	vis	3
44458.426	-2604	+0.003	vis	4
44458.439	-2604	+0.016	vis	4
44490.354	-2549	+0.008	vis	5
44490.355	-2549	+0.009	vis	5
45612.323	-616	-0.001	vis	6
45969.8604	0	-0.0105	pe	This study
46298.388	+566	-0.008	vis	7

* The O-C values are calculated with the ephemeris: Min I = HJD2445969.8709 + 0.58043326 E.
** Sources. 1: Jensch 1935, 2: Whitney 1957, 3: BBSAG (Bedeckungsveränderlichen Beobachter der Schweizerischen Astronomischen Gesellschaft) Bull., No.45 (1979), 4: BBSAG Bull., No.49 (1980), 5: BBSAG Bull., No.50 (1980), 6: BBSAG Bull., No.69 (1983), 7: BBSAG Bull., No.78 (1985).

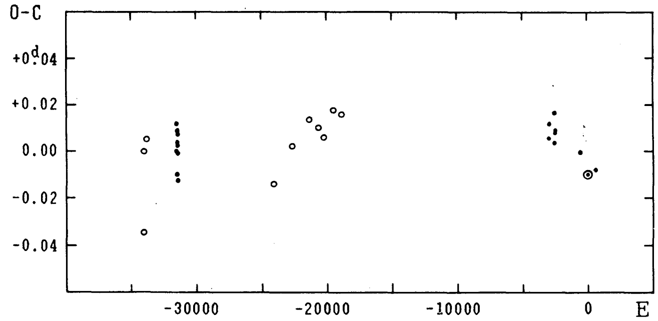

FIG. 1–($O-C$) values of times of minima of BO Peg. Dots, open circles, and dot-open circle denote visual, photographic, and photoelectric observations, respectively.

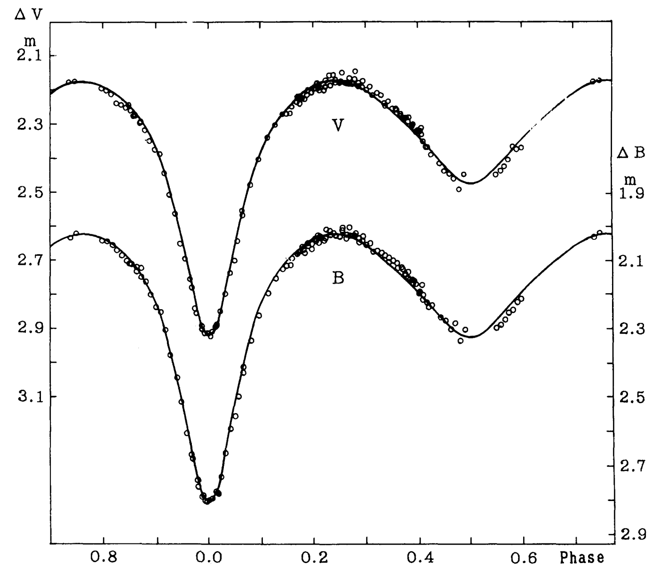

FIG. 2–Light variations of BO Peg in V and B. Theoretical curves are shown with solid curves.

variable minus comparison, are given in Appendix Table A1, where phases are calculated using the ephemeris

$$\text{Min. I} = \text{HJD } 2445969.8604 + 0.58043288\, E \ ,$$

which was derived by adopting the time of the primary minimum obtained in this study as the epoch. The light variations in V and B are also shown in Figure 2. It is obvious that this system suffers large proximity effects.

III. Light-Curve Analysis

We analyzed the BV light curves using the light-curve synthesis method developed by one of us (A.Y.). In this method, the photospheric configurations of the components are approximated by the Roche equipotential surfaces (e.g., Yamasaki, Okazaki, and Kitamura 1983).

In the present analysis, the surfaces of the primary and secondary components were divided into 994 and 582 elements, respectively. The envelope of the primary component was assumed to be radiative and that of the secondary component to be convective. We adopted the following values throughout the analysis:

	Primary	Secondary
Limb-darkening coefficient:	$u_{1V} = 0.56$	$u_{2V} = 0.60$
	$u_{1B} = 0.68$	$u_{2B} = 0.74$
Gravity-darkening exponent:	$\beta_1 = 0.25$	$\beta_2 = 0.08$
Albedo:	$A_1 = 1.0$	$A_2 = 0.5$,

where the linear limb-darkening coefficients of the primary component are for an ~ F0-type star and those of the secondary component are for an ~ G0-type star (Carbon and Gingerich 1969).

The system parameters have been obtained by minimizing $(O-C)^2 = \Sigma_i\,(l_{\rm obs}-l_{\rm th})_i^{\,2}$, where the summation is over all observations. Table III gives the final solution of the system parameters for BO Peg. Theoretical light curves computed with these parameters are shown for V and B in Figure 2 with solid curves.

Figure 3 represents the configurations of the components of BO Peg relative to their critical Roche lobes. It is shown that the components are not in contact with each

TABLE III

System Parameters of BO Peg

Mass ratio: q		0.55 ±0.05
Inclination: i		$79^\circ.1 \pm 1^\circ.0$
Fractional radius of the primary component: r_1	side	0.430 ±0.010
	substellar	0.545
	back	0.458
	pole	0.406
(Roche,	side	0.431)
Fractional radius of the secondary component: r_2	side	0.310 ±0.010
	substellar	0.373
	back	0.337
	pole	0.298
(Roche,	side	0.321)
Fractional luminosity of the primary component: L_1	V	0.914 ±0.020
	B	0.919 ±0.020
Fractional luminosity of the secondary component: L_2	V	0.086 ±0.020
	B	0.081 ±0.020

other, although they almost fill their critical Roche lobes—the primary component fills its critical Roche lobe and the secondary component is very close to its critical lobe.

IV. Spectroscopic Observations

We secured two spectrograms of BO Peg with a dispersion of 32 Å mm^{-1} with the coudé image-tube spectrograph of the 1.9-m reflector at Okayama Astrophysical Observatory in November 1980. These spectrograms were taken outside eclipses on HJD2444545.008 ($0^{\rm P}.190$) and HJD2444547.067 ($0^{\rm P}.737$). No emission features were detected in these spectrograms. The spectral type of BO Peg outside eclipses was determined to be A7 IV–V or slightly later.

V. Discussion

To deduce reliable absolute dimensions of BO Peg, radial-velocity observations are essential; however, it is not practical to make discussions with only two spectrograms. Therefore, in the following discussions, we assume the mass of the primary component $\mathfrak{M}_1 = 1.9\,\mathfrak{M}_\odot$ corresponding to the spectral type of A7 IV–V (Allen 1973). From the system parameters given in Table III, we obtain:

Mass of the primary component:	$\mathfrak{M}_1 = 1.9\,\mathfrak{M}_\odot$	(assumed)
Mass of the secondary component:	$\mathfrak{M}_2 = 1.0\,\mathfrak{M}_\odot$	
Radius of the primary component:	$R_1 = 1.8\,R_\odot$	
Radius of the secondary component:	$R_2 = 1.3\,R_\odot$	
Separation:	$A = 4.2\,R_\odot$.	

Both components of BO Peg are found to have radii slightly larger than those of corresponding main-sequence stars of the same masses. The secondary component is considered to be an early-G-type star from its mass.

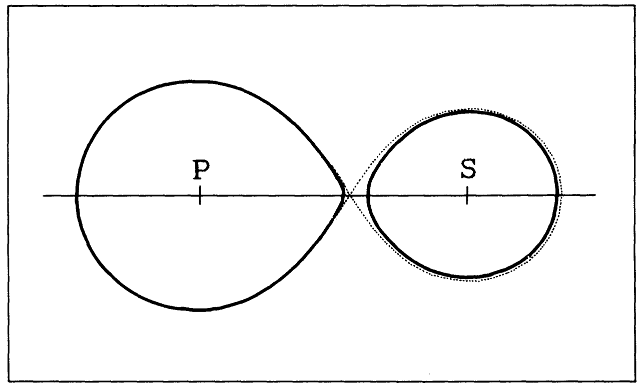

FIG. 3–Configurations of the components of BO Peg (solid line) relative to their critical Roche lobes (dotted line). P and S represent the centers of the primary and the secondary components, respectively.

According to the light-curve analysis in Section III, the components are not in contact, although they are very close to each other. From the fractional luminosities and radii in Table III, the brightness ratio J_1/J_2 was derived to be 5.5–5.9. The large brightness ratio also suggests that the system of BO Peg does not have a common envelope.

In conclusion, BO Peg is a new member of short-period noncontact binary systems (Yamasaki *et al.* 1983; Yamasaki, Okazaki, and Kitamura 1984), or almost contact systems, in which interacting-binary evolution off the main sequence has just taken place.

We would like to thank Professor D. N. B. Hall, Director, Professor J. P. Henry, and the staff of the University of Hawaii at Mauna Kea Observatory. We are grateful to Dr. J. Goguen for the photometric system. We also thank the staff of the Okayama Astrophysical Observatory. This work was supported by the Grant-in-Aid for Overseas Scientific Survey (59041022, 60043023) of the Ministry of Education, Science, and Culture of Japan.

REFERENCES

Allen, C. W. 1973, *Astrophysical Quantities* (3d ed.; London: Athlone Press), p. 209.

Carbon, D. F., and Gingerich, O. 1969, in *Theory and Observation of Normal Stellar Atmospheres*, ed. O. Gingerich (Cambridge, MA: MIT Press), p. 377.

Goguen, J. 1984, unpublished.

Hoffmeister, C. 1935, *Astr. Nach.*, **255**, 401.

Jensch, A. 1935, *Astr. Nach.*, **255**, 417.

Kukarkin, B. V., *et al.* 1971, *First Supplement to the Third Edition of the General Catalogue of Variable Stars* (Moscow: Academy of Sciences of the USSR).

Whitney, B. S. 1957, *A.J.*, **62**, 371.

Yamasaki, A., Okazaki, A., and Kitamura, M. 1983, *Pub. Astr. Soc. Japan*, **35**, 131.

———. 1984, *Pub. Astr. Soc. Japan*, **36**, 175.

TABLE A1

Photoelectric Observations of BO Peg

HJD 2445000+	Phase	ΔV
958.8432	0.0190	2.891
958.8630	0.0530	2.706
958.8720	0.0687	2.572
958.8805	0.0833	2.480
958.8891	0.0981	2.407
958.8991	0.1152	2.341
958.9070	0.1289	2.305
958.9152	0.1431	2.273
958.9238	0.1579	2.271
958.9322	0.1724	2.222
958.9397	0.1852	2.230
958.9474	0.1984	2.210
958.9553	0.2121	2.198
958.9632	0.2258	2.173
958.9715	0.2400	2.158
958.9811	0.2565	2.152
958.9886	0.2696	2.167
958.9960	0.2822	2.149
959.0038	0.2957	2.177
959.0289	0.3390	2.248
967.7597	0.3809	2.281
967.7663	0.3921	2.309
967.7758	0.4085	2.313
967.7825	0.4201	2.370
969.7429	0.7976	2.195
969.7485	0.8072	2.201
969.7539	0.8166	2.212
969.7593	0.8258	2.238
969.7648	0.8352	2.242
969.7701	0.8444	2.251
969.7755	0.8537	2.260
969.7807	0.8627	2.272
969.7864	0.8725	2.292
969.8441	0.9718	2.784
969.8493	0.9808	2.859
969.8547	0.9902	2.896
969.8604	0.0001	2.919
969.8657	0.0091	2.914
969.8698	0.0161	2.896
969.8752	0.0255	2.855
969.8808	0.0351	2.802
969.8861	0.0442	2.740
969.8939	0.0578	2.646
969.8994	0.0672	2.557
969.9477	0.1504	2.271
969.9536	0.1606	2.250
969.9592	0.1702	2.237
969.9647	0.1798	2.224
969.9707	0.1901	2.216
969.9790	0.2044	2.200
969.9846	0.2139	2.204
969.9907	0.2245	2.191
969.9965	0.2344	2.188
970.0022	0.2443	2.173
970.0133	0.2635	2.181
970.0207	0.2762	2.185
970.0274	0.2877	2.182
970.8680	0.7359	2.176
970.8742	0.7466	2.174
970.9339	0.8496	2.244
970.9402	0.8604	2.273
970.9415	0.8626	2.275
970.9469	0.8718	2.296
970.9522	0.8810	2.317
970.9581	0.8912	2.348
970.9634	0.9003	2.374
970.9687	0.9094	2.388
970.9743	0.9191	2.445
970.9800	0.9289	2.508
970.9865	0.9401	2.564
970.9921	0.9498	2.653
970.9980	0.9599	2.698

HJD 2445000+	Phase	ΔV
971.0034	0.9692	2.759
971.0091	0.9790	2.846
971.0166	0.9920	2.907
971.0198	0.9975	2.916
971.0225	0.0021	2.918
971.0267	0.0094	2.927
971.0326	0.0196	2.895
971.7236	0.2100	2.181
971.7312	0.2232	2.202
971.7483	0.2525	2.179
971.7552	0.2645	2.182
971.7600	0.2727	2.183
971.7640	0.2797	2.171
971.7687	0.2878	2.192
971.7730	0.2951	2.194
971.7769	0.3019	2.202
971.7809	0.3087	2.192
971.7850	0.3158	2.218
971.7892	0.3230	2.211
971.7937	0.3308	2.217
971.7976	0.3375	2.241
971.8018	0.3448	2.234
971.8059	0.3519	2.256
971.8117	0.3617	2.258
971.8164	0.3698	2.272
971.8202	0.3764	2.280
971.8241	0.3832	2.282
971.8282	0.3902	2.305
971.8322	0.3971	2.323
971.8364	0.4044	2.323
971.8405	0.4115	2.353
971.9222	0.5521	2.450
971.9272	0.5608	2.441
971.9313	0.5679	2.427
971.9356	0.5753	2.408
971.9400	0.5828	2.369
971.9446	0.5907	2.376
971.9489	0.5982	2.372
972.8644	0.1754	2.240
972.8687	0.1828	2.224
972.8730	0.1903	2.208
972.8774	0.1979	2.208
972.8820	0.2058	2.196
972.8864	0.2133	2.187
972.8973	0.2321	2.157
972.9043	0.2442	2.178
972.9110	0.2557	2.174
972.9713	0.3596	2.256
972.9762	0.3681	2.276
972.9805	0.3755	2.288
972.9850	0.3832	2.293
972.9897	0.3913	2.303
972.9955	0.4013	2.320
972.9998	0.4087	2.331
973.0046	0.4169	2.370
973.0101	0.4264	2.392
973.0197	0.4429	2.420
973.0249	0.4520	2.442
973.0307	0.4619	2.449
973.0355	0.4702	2.463
973.0412	0.4801	2.495
973.0468	0.4896	2.451

HJD 2445000+	Phase	ΔB
958.8442	0.0207	2.782
958.8638	0.0545	2.557
958.8730	0.0704	2.428
958.8815	0.0850	2.335

HJD 2445000+	Phase	ΔB
958.8901	0.0998	2.262
958.9001	0.1170	2.196
958.9080	0.1307	2.154
958.9163	0.1449	2.125
958.9248	0.1596	2.113
958.9332	0.1741	2.073
958.9407	0.1870	2.078
958.9484	0.2002	2.065
958.9563	0.2139	2.048
958.9642	0.2274	2.009
958.9725	0.2418	2.019
958.9820	0.2582	2.004
958.9897	0.2714	2.002
958.9971	0.2841	2.018
959.0048	0.2974	2.028
959.0323	0.3448	2.104
967.7607	0.3826	2.134
967.7681	0.3953	2.161
967.7768	0.4102	2.172
967.7836	0.4219	2.238
969.7439	0.7993	2.041
969.7495	0.8089	2.042
969.7549	0.8183	2.053
969.7603	0.8276	2.069
969.7657	0.8369	2.084
969.7711	0.8461	2.100
969.7764	0.8554	2.109
969.7817	0.8644	2.119
969.7874	0.8742	2.122
969.8450	0.9735	2.684
969.8502	0.9824	2.746
969.8557	0.9919	2.794
969.8615	0.0018	2.806
969.8666	0.0108	2.800
969.8707	0.0178	2.781
969.8762	0.0272	2.735
969.8817	0.0368	2.667
969.8870	0.0459	2.595
969.8949	0.0594	2.500
969.9004	0.0689	2.413
969.9487	0.1521	2.118
969.9545	0.1622	2.094
969.9602	0.1719	2.080
969.9657	0.1815	2.060
969.9718	0.1919	2.049
969.9800	0.2060	2.036
969.9856	0.2156	2.028
969.9917	0.2262	2.035
969.9975	0.2361	2.024
970.0032	0.2460	2.027
970.0143	0.2651	2.024
970.0217	0.2778	2.026
970.0284	0.2894	2.046
970.8690	0.7376	2.031
970.8752	0.7483	2.019
970.9349	0.8513	2.106
970.9425	0.8643	2.133
970.9478	0.8735	2.149
970.9532	0.8827	2.163
970.9591	0.8929	2.202
970.9644	0.9020	2.237
970.9696	0.9111	2.253
970.9753	0.9208	2.306
970.9810	0.9307	2.377
970.9875	0.9418	2.444
970.9931	0.9514	2.517
970.9989	0.9614	2.608
971.0044	0.9709	2.670
971.0118	0.9836	2.768
971.0176	0.9937	2.793
971.0188	0.9958	2.810
971.0235	0.0038	2.807

HJD 2445000+	Phase	ΔB
971.0336	0.0213	2.788
971.7246	0.2117	2.025
971.7322	0.2249	2.038
971.7492	0.2541	2.026
971.7561	0.2660	2.033
971.7607	0.2739	2.025
971.7648	0.2810	2.024
971.7695	0.2891	2.033
971.7736	0.2962	2.040
971.7776	0.3031	2.051
971.7816	0.3099	2.047
971.7858	0.3171	2.073
971.7900	0.3244	2.069
971.7944	0.3321	2.073
971.7983	0.3388	2.083
971.8026	0.3461	2.088
971.8067	0.3531	2.098
971.8119	0.3622	2.120
971.8170	0.3710	2.122
971.8209	0.3776	2.136
971.8249	0.3845	2.149
971.8289	0.3915	2.154
971.8330	0.3985	2.170
971.8371	0.4055	2.191
971.8410	0.4122	2.200
971.9228	0.5532	2.297
971.9278	0.5619	2.287
971.9321	0.5693	2.271
971.9363	0.5764	2.252
971.9408	0.5841	2.242
971.9452	0.5919	2.220
971.9496	0.5994	2.212
972.8651	0.1767	2.072
972.8695	0.1841	2.068
972.8738	0.1916	2.055
972.8782	0.1992	2.053
972.8827	0.2070	2.041
972.8871	0.2146	2.035
972.8981	0.2335	2.012
972.9051	0.2456	2.027
972.9117	0.2569	2.009
972.9720	0.3608	2.107
972.9770	0.3694	2.121
972.9813	0.3768	2.143
972.9858	0.3846	2.154
972.9904	0.3925	2.168
972.9962	0.4025	2.196
973.0006	0.4100	2.215
973.0053	0.4183	2.225
973.0108	0.4276	2.231
973.0204	0.4442	2.266
973.0257	0.4533	2.276
973.0314	0.4632	2.303
973.0362	0.4715	2.285
973.0422	0.4817	2.337
973.0477	0.4912	2.304

HJD 2445000+	Phase	ΔU
958.8454	0.0228	2.819
959.0334	0.3466	2.304
971.7332	0.2266	2.054
971.7501	0.2557	2.052
972.8989	0.2349	2.064
972.9059	0.2469	2.063
972.9124	0.2581	2.066